tion depends only on the probability score and the sample-of-N climatological probability of adverse weather. In addition, an expression has been obtained for this situation which indicates the range of values of the probability score for which the predictions are of greater utility than climatological predictions.

The relationship between the natural measure of the "value" of probabilistic predictions, i.e., utility, and artificial measures of the "value" of probabilistic predictions, e.g., the probability score, for cost-loss ratio decision situations in which knowledge of the decision maker's utilities assumes different forms and for more complex decision situations is considered elsewhere (Murphy, 1966).

REFERENCES

Brier, G. W., 1950: Verification of forecasts expressed in terms of probability. *Mon. Wea. Rev.*, **78**, 1–3.

Epstein, E. S., and A. H. Murphy, 1965: A note on the attributes of probabilistic predictions and the probability score. *J. Appl. Meteor.*, **4**, 297–299.

Fishburn, P. C., 1964: *Decision and Value Theory*. New York, John Wiley and Sons, 451 pp.

Luce, R. D., and H. Raiffa, 1957: *Games and Decisions*. New York, John Wiley and Sons, 509 pp.

Murphy, A. H., 1966: The evaluation of probabilistic predictions in the atmospheric sciences: two strategy-two state of nature decision situation. Ann Arbor, The University of Michigan, Department of Meteorology and Oceanography, Contract Number Cwb-10847, Technical Report 5-T. (Available from the author.)

The Effect of Atmospheric Lapse Rates on Balloon Ascent Rates

RALPH D. REYNOLDS

Atmospheric Science Office, White Sands Missile Range, N. Mex.

4 May 1965 and 30 March 1966

1. Introduction

The position of an ascending balloon can be approximated by a consideration of the wind field through which it passes and the speed of its ascent. The wind field can be fairly well described through forecasting techniques. Balloon ascent rate can be estimated from a consideration of the amount of free lift given the balloon in the inflation calculations, the aerodynamic drag relationships of the balloon system and the temperature lapse rate. This report is concerned primarily with the effect of temperature lapse rate on the ascent rate. The large number of radar-tracked skyhook balloon trajectories, together with timely rawinsonde data, available at White Sands Missile Range (WSMR) made the study of this relationship possible.

2. Background

Ascent rates differing substantially from the expected mean rate of 850 ft min^{-1} have been noted in positioning large, non-extensible, polyethylene balloon systems over specified target areas and within strict altitude and time limits at WSMR.

In studies of skyhook balloons, their design and relationship to atmospheric parameters (University of Minnesota, 1952), it was found that the amount of energy which must be transferred to a rising balloon to maintain its ascent is a function of the temperature lapse rate. In these studies of balloon thermodynamics, the following equation was developed:

$$P=(0.65L+2.6)GV, \tag{1}$$

where

L = lapse rate in °C (1000 ft)$^{-1}$,
G = gross load in units of 100 lb,
V = velocity in units of 1000 ft min^{-1} (ascent rate),
P = power in kw.

The physical relationship of the lapse rate and the power of a balloon may best be understood if the balloon is considered as a heat engine. Heat is transferred to a balloon gas by convection from the balloon fabric, direct absorption of sunlight or infrared radiation and by the work the gas does against atmospheric pressure as the balloon ascends (Greenfield and Davis, 1963). Greenfield and Davis consider convection to be the most important method of heat transfer.

3. Approach

On some of the research balloon flights from WSMR, Eq. (1) gave seemingly accurate indications of changes in ascent rate due to changes in temperature lapse rate[1]. Using this relationship to test sporadic samples,

[1] B. D. Gildenberg, private communication, 1961.

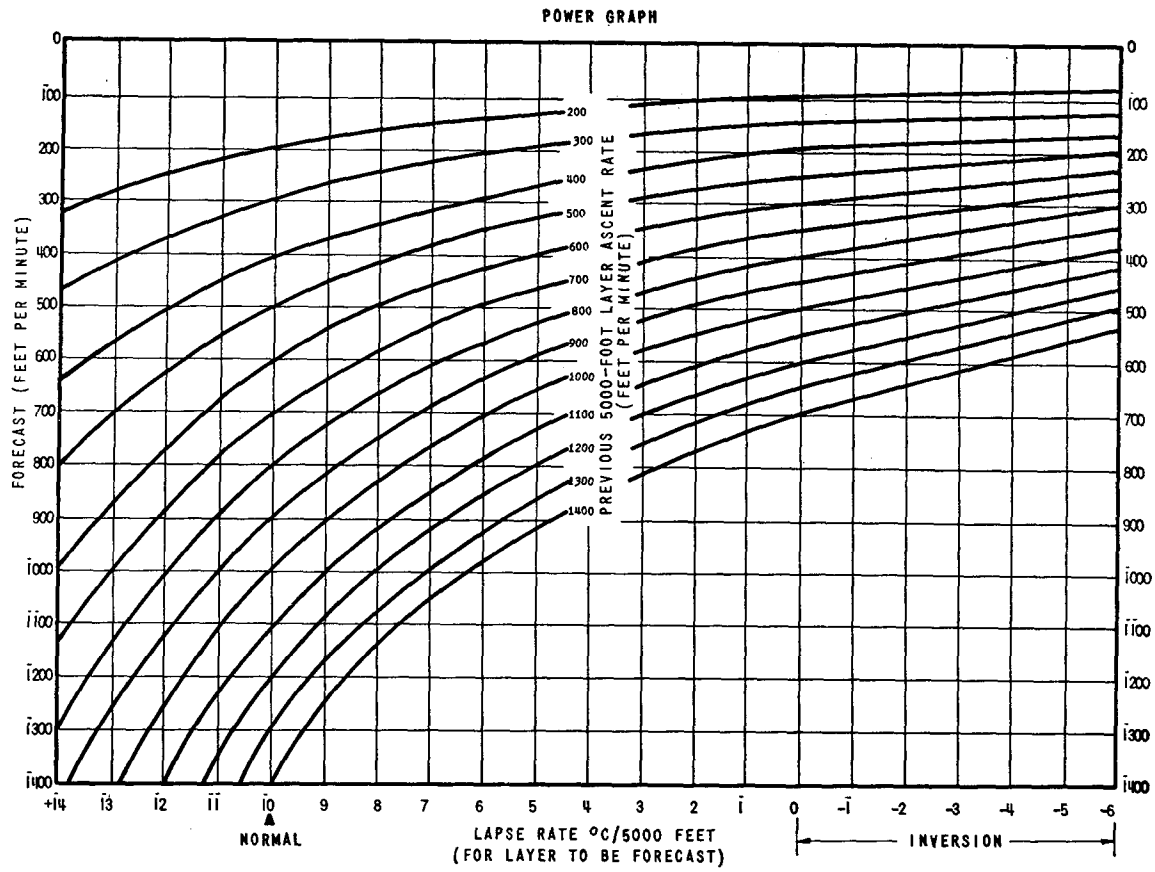

FIG. 1. The power graph, a nomogram solution of Eq. (1). The power graph is entered with the average lapse rate for the 5000-ft level to be forecast plus the previous 5000-ft layer ascent rate. The resultant forecast is read out on the ordinate.

Gildenberg thought that (1) would yield results accurate to within plus or minus 50 ft min^{-1} for the large skyhook balloons.

Eq. (1) initially provided a means for predicting ascent rates from temperature lapse rates. To check the accuracy of the equation, it was decided to compare the computed ascent rates with the observed rates. A power graph (Fig. 1) based on (1) was prepared to facilitate computations. This was done by solving the equation for a given power value using the normal lapse rate of $-10C\ (5000\ ft)^{-1}$, a gross load of 2000 pounds (based on the average gross load of the radar-tracked data used in this study) and an assumed ascent rate of 1000 ft min^{-1}. The power value is then held constant and the lapse rate varied to yield one curve.

Similarly, a family of curves is developed by finding the power for an initial assumed ascent rate and the normal lapse rate, and then holding the power value constant for that particular curve as the lapse rate is varied and the associated ascent rate V determined.

Thus, Eq. (1) becomes

$$V_{1000}=P[1000\ \text{ft min}^{-1};\ -10C\ (5000\ \text{ft})^{-1}]/(0.65L+2.6)20, \quad (2)$$

$$V_{900}=P[900\ \text{ft min}^{-1};\ -10C\ (5000\ \text{ft})^{-1}]/(0.65L+2.6)20, \quad (3)$$

and similarly for other values.

One of the parameters involved in the use of both (1) and the power graph is the average ascent rate V in the lower stratum adjacent to the layer to be forecast, that is, the ascent rate in this lower stratum is used to compensate for the momentum of the large balloon systems as they ascend through different lapse rate areas aloft. For example, a balloon ascending at 1100 ft min^{-1} through an area of steep lapse rates and then suddenly entering an inversion cannot be expected to respond instantaneously to the new lapse rate.

4. Results

To test the power graph for non-extensible balloons, AN/FPS-16 radar records of 50 flights from Holloman Air Force Base, New Mexico, during 1961 and 1962, were used. These flights were randomly distributed throughout the year. The height-time information was extracted from plotting board data using time intervals to the nearest quarter-minute, and balloon heights

BALLOON

FLIGHT DATA

TIME SECONDS	X AXIS POS. FEET	X AXIS VEL. FT/SEC.	X AXIS ACCEL. G,S	Y AXIS POS. FEET	Y AXIS VEL. FT/SEC.	Y AXIS ACCEL. G,S	Z AXIS POS. FEET	Z AXIS VEL. FT/SEC.	Z AXIS ACCEL. G,S	TANGENTIAL VEL. FT/SEC.	TANGENTIAL ACCEL. G,S	ALTITUDE MSL FEET
5534.0	99590	5	.0	3231	166	.0	40909	6	.0	166	.0	41146
5535.0	99589	5	.0	3399	166	.0	40915	7	.0	166	.0	41152
5536.0	99585	5	.0	3560	166	.0	40917	7	.0	166	.0	41155
5537.0	99617	6	.0	3738	166	.0	40935	7	.0	167	.0	41172
5538.0	99633	6	.0	3902	166	.0	40946	7	.0	167	.0	41184
5539.0	99623	6	.0	4066	167	.0	40943	7	.0	167	.0	41180
5540.0	99616	6	.0	4231	167	.0	40945	7	.0	167	.0	41182
5541.0	99621	6	.0	4394	167	.0	40953	7	.0-	167	.0	41190
5542.0	99644	6	.0-	4571	167	.0-	40969	7	.0-	167	.0-	41206
5543.0	99630	6	.0-	4737	167	.0-	40970	7	.0-	167	.0-	41208
5544.0	99674	6	.0-	4896	167	.0-	40995	7	.0-	167	.0-	41233
5545.0	99654	6	.0-	5069	167	.0-	40990	7	.0-	167	.0-	41228
5546.0	99676	5	.0-	5234	166	.0-	41005	6	.0-	167	.0-	41243
5547.0	99671	5	.0-	5401	167	.0-	41002	6	.0-	167	.0-	41240
5548.0	99675	6	.0-	5573	167	.0-	41012	6	.0-	167	.0-	41250
5549.0	99668	6	.0-	5734	167	.0	41004	6	.0-	167	.0	41242
5550.0	99690	6	.0	5896	167	.0	41021	6	.0-	167	.0	41259
5551.0	99683	6	.0	6065	167	.0	41017	6	.0	167	.0	41255
5552.0	99684	6	.0	6237	167	.0	41025	6	.0	167	.0	41263
5553.0	99703	6	.0	6400	167	.0	41037	6	.0	167	.0	41275
5554.0	99714	6	.0	6556	167	.0	41045	6	.0	167	.0	41283
5555.0	99697	7	.0	6729	167	.0	41043	6	.0	167	.0	41281
5556.0	99709	7	.0	6897	167	.0	41054	6	.0	167	.0	41293
5557.0	99728	8	.0	7068	167	.0	41062	7	.0	167	.0	41301
5558.0	99743	9	.0	7244	167	.0	41072	7	.0	168	.0	41311
5559.0	99738	9	.0	7400	167	.0-	41073	7	.0	168	.0-	41312
5560.0	99752	9	.0	7575	167	.0-	41084	7	.0	168	.0-	41323
5561.0	99756	10	.0	7738	167	.0-	41083	7	.0	167	.0-	41322
5562.0	99771	9	.0	7902	167	.0-	41092	7	.0-	167	.0-	41331
5563.0	99775	9	.0-	8071	167	.0-	41098	7	.0-	167	.0-	41337
5564.0	99789	10	.0-	8238	166	.0-	41105	7	.0-	167	.0-	41345

FIG. 2. A sample of the cinetheodolite position and velocity data taken of a balloon ascent on 15 December 1964. This is only one page of the 213 pages of data for this balloon's ascent from 30,000 ft to its float altitude of 107,000 ft. The column on the right is the altitude above mean sea level which has been corrected for the curvature of the earth.

were corrected for refraction and earth curvature (U. S. Coast and Geodetic Survey, 1921). The maximum error using this procedure is ± 20 ft min^{-1} (Angell and Pack, 1962).

The recorded temperature data from the rawinsonde nearest to the time of release of the research balloon were used, all being within ± 2 hr of the release of the non-extensible balloons.

A sample of some more recent data which utilized cinetheodolite data, computer reduced for a minimum of three stations, is shown in Fig. 2. The radiosonde record from an instrument launched simultaneously with the non-extensible balloon is shown in Fig. 3.

The computed ascent rate was correlated with the observed rate for 5000-ft layers between 10,000 and 100,000 ft MSL. The resulting correlation coefficients and standard errors for the power graph method are listed in Table 1. Because of the correlation coefficients and relatively large values of the standard errors, a statistical relationship between observed lapse rate and ascent rate was investigated to try to reduce the large standard errors. This statistical correlation was based on a mean ascent rate of 850 ft min^{-1} from the surface to 100,000 feet MSL. Using all the data, the ascent rate of non-extensible balloons was correlated with lapse rate for 5000-ft layers between 10,000 and 100,000 feet

TABLE 1. Correlation coefficients between observed ascent rates and those computed by the power graph method and the standard error in ascent rates for the power graph method at 5000-ft intervals between 10,000 and 100,000 ft for polyethylene balloons.

Number of samples	Altitude (thousands of feet)	Correlation coefficient	Standard error (ft min^{-1})
48	10–15	+0.527	220
47	15–20	+0.338	190
48	20–25	+0.468	200
47	25–30	+0.536	180
49	30–35	+0.319	230
46	35–40	+0.181	240
44	40–45	+0.519	190
45	45–50	+0.310	250
41	50–55	+0.268	190
38	55–60	+0.286	280
22	60–65	+0.577	180
22	65–70	+0.224	270
22	70–75	+0.137	350
22	75–80	+0.099	240
22	80–85	−0.307	380
22	85–90	+0.068	360
17	90–95	+0.494	430
15	95–100	+0.303	310

UPPER AIR DATA

STATION ALTITUDE 4090FEET MSL
DATE 15 DEC 1964, 0735 HRS MST
ASCENSION NO.387.

HOLLOMAN SITE

WSTM SITE COORDINATES
E 575,700 FEET
N 352,000 FEET

GEOMETRIC ALTITUDE MSL FEET	PRESSURE MILLIBARS	TEMPERATURE AIR DEGREES CENTIGRADE	TEMPERATURE DEWPOINT CENTIGRADE	RELATIVE HUMIDITY PERCENT	DENSITY GM/CUBIC METER	SPEED OF SOUND KNOTS	WIND DATA DIRECTION DEGREES(TN)	WIND DATA SPEED KNOTS	INDEX OF REFRACTION	Flight Time, Minutes
37000.	217.8	-54.2			346.5	576.	256.	95.	1.000077	51.7
37200.	215.7	-54.3			343.3	576.	255.	97.	1.000076	
37400.	213.7	-54.4			340.3	576.	254.	98.	1.000076	
37600.	211.6	-54.8			337.7	575.	253.	100.	1.000075	
37800.	209.6	-55.2			335.1	575.	253.	101.	1.000075	
38000.	207.7	-55.6			332.5	574.	253.	103.	1.000074	53.0
38200.	205.7	-55.9			329.9	574.	252.	105.	1.000073	
38400.	203.7	-56.3			327.3	573.	252.	106.	1.000073	
38600.	201.8	-56.6			324.7	573.	254.	109.	1.000072	
38800.	199.9	-57.0			322.2	572.	255.	111.	1.000072	
39000.	198.0	-57.3			319.6	572.	256.	113.	1.000071	54.3
39200.	196.1	-57.7			317.1	572.	258.	115.	1.000071	
39400.	194.2	-57.4			313.6	572.	260.	117.	1.000070	
39600.	192.3	-57.1			310.2	572.	262.	118.	1.000069	
39800.	190.5	-56.9			306.9	573.	264.	118.	1.000068	
40000.	188.7	-56.6			303.5	573.	265.	118.	1.000068	56.1
40200.	186.9	-56.3			300.3	573.	267.	118.	1.000067	
40400.	185.1	-56.0			297.0	574.	267.	114.	1.000066	
40600.	183.4	-55.7			293.8	574.	267.	111.	1.000065	
40800.	181.6	-55.3			290.4	575.	266.	108.	1.000065	
41000.	179.9	-54.3			286.4	576.	264.	105.	1.000064	58.0
41200.	178.2	-54.4			283.9	576.	263.	101.	1.000063	
41400.	176.5	-54.6			281.4	576.	262.	100.	1.000063	
41600.	174.9	-55.0			279.2	575.	262.	99.	1.000062	
41800.	173.2	-55.3			277.1	575.	261.	98.	1.000062	
42000.	171.6	-55.7			274.9	574.	262.	98.	1.000061	59.7
42200.	169.9	-56.1			272.7	574.	263.	98.	1.000061	
42400.	168.3	-56.4			270.6	573.	264.	98.	1.000060	
42600.	166.7	-56.8			268.5	573.	266.	98.	1.000060	
42800.	165.1	-57.2			266.4	572.	268.	99.	1.000059	
43000.	163.5	-57.6			264.3	572.	270.	99.	1.000059	61.2
43200.	162.0	-57.9			262.2	571.	272.	100.	1.000058	
43400.	160.4	-58.3			260.2	571.	274.	100.	1.000058	

FIG. 3. A sample of the computer-reduced radiosonde data that corresponds to the same height range shown in Fig. 2. The radiosonde was released simultaneously with the release of the skyhook balloon.

MSL. The correlation coefficients and standard errors of these correlations are listed in Table 2. With minor exceptions, the results do not differ appreciably from those in Table 1. Seasonal effects and change in tropopause heights were also investigated in the correlation of lapse rate with ascent rate but yielded results which were not significantly different from those when all data were combined.

TABLE 2. Correlation coefficients between observed ascent rates and lapse rates and the standard error in ascent rates at 5000-ft intervals between 10,000 and 100,000 ft for polyethylene balloons.

Number of samples	Altitude (thousands of feet)	Correlation coefficient	Standard error (ft min^{-1})
48	10–15	+0.400	220
49	15–20	+0.137	240
48	20–25	+0.372	280
49	25–30	+0.116	200
49	30–35	+0.284	250
47	35–40	+0.227	240
46	40–45	+0.249	240
47	45–50	+0.221	280
43	50–55	−0.122	210
41	55–60	+0.207	290
22	60–65	+0.273	260
22	65–70	+0.257	250
22	70–75	−0.155	320
22	75–80	−0.026	250
22	80–85	+0.189	350
22	85–90	−0.098	400
17	90–95	−0.011	290
15	95–100	+0.331	280

The same procedure used for non-extensible balloons was used for neoprene balloons and the resulting correlation coefficients and standard errors are shown in Tables 3 and 4. The neoprene balloon data were taken from radar magnetic tape from the AN/FPS-16 radar which was computer reduced and are accurate to ±1 ft min^{-1}.

For polyethylene balloons and the power graph, the largest correlation ($r=0.577$) was found between 60,000 and 65,000 ft. The average correlation coefficient of +0.394 was found for the stratum from 10,000 to 65,000 ft. Thus, the coefficient of determination (r^2) for this study shows that only 16 per cent of the ascent rate factor may be attributed to temperature lapse rates between 10,000 and 65,000 ft. The average correlation coefficient between 10,000 and 100,000 ft was +0.297 with $r^2=0.09$; thus only 9 per cent of ascent rate variation is attributable to the lapse rate factor.

5. Conclusions

The effect of lapse rate on the ascent rate of non-extensible and neoprene balloons tested here has been

TABLE 3. Correlation coefficients between observed ascent rates and those computed by the power graph method and the standard error in ascent rates for the power graph method at 5000-ft intervals between 10,000 and 60,000 ft for neoprene balloons.

Number of samples	Altitude (thousands of feet)	Correlation coefficient	Standard error (ft min^{-1})
	10–15	*	*
25	15–20	+0.195	96
25	20–25	−0.331	104
25	25–30	+0.940	162
25	30–35	+0.108	97
25	35–40	+0.677	107
24	40–45	+0.323	102
23	45–50	+0.127	106
23	50–55	+0.400	163
23	55–60	+0.023	114

* Incomplete data.

found to be relatively small. Only 9 per cent of the variation in ascent rate may be attributed to the lapse rate between 10,000 and 100,000 ft for polyethylene balloons and 8 per cent for neoprene balloons to 60,000 ft. This suggests that other factors such as convection and radiation have greater effects on balloon ascent rates. Until the state-of-the-art has advanced concerning the other factors involved in the ascent rate of balloons, the temperature lapse rate effects may be neglected.

TABLE 4. Correlation coefficients between observed ascent rates and lapse rates and the standard error in ascent rates at 5000-ft intervals between 10,000 and 60,000 ft for neoprene balloons.

Number of samples	Altitude (thousands of feet)	Correlation coefficient	Standard error (ft min^{-1})
	10–15	*	*
25	15–20	+0.867	98
25	20–25	−0.233	65
25	25–30	−0.098	65
25	30–35	−0.096	102
25	35–40	+0.672	88
25	40–45	+0.013	115
23	45–50	+0.101	129
23	50–55	+0.139	158
23	55–60	−0.246	100

* Incomplete data.

REFERENCES

Angell, J. K., and D. H. Pack, 1962: Analysis of low-level constant volume balloon flights from Wallops Island. *J. Atmos. Sci.*, **19**, 87–98.

Campen, C. F., Jr. *et al.*, 1960: Balloon Systems. *Handbook of Geophysics*, New York, Macmillan, Chapter 20, 40–43.

Greenfield, S. M., and M. H. Davis, 1963: The physics of balloons and their feasibility as exploration vehicles on Mars. The RAND Corporation, Santa Monica, Calif., R-421-JPL, 115–123.

University of Minnesota, 1952: Thermodynamics of a balloon. *Balloon Physics*, Vol. I, Chapter IV, Department of Physics, University of Minnesota, 60–63.

U. S. Coast and Geodetic Survey, 1921: Special Publication No. 26. U. S. Government Printing Office, Washington, D. C., 8–10.

Comments on the Accuracy of TIROS Hurricane Locations

NEIL L. FRANK

National Hurricane Center, Miami, Fla.

31 August 1965 and 21 December 1965

1. Introduction

In a recent article, Hubert and Timchalk (1964) discussed the accuracy of TIROS hurricane locations. They compared estimates made from TIROS pictures with operational aircraft reconnaissance fixes. A slightly different comparison was made on Atlantic tropical storms during the past two summers (1963–1964) at the National Hurricane Center. The approach differs from the earlier study in two ways: 1) the "best track" was used as a standard rather than aircraft positions, and 2) weaker storms were considered, i.e., tropical storms and depressions.

The "best track" for each storm is determined after the hurricane season utilizing the complete collection of data. The objective is to minimize either random or systematic errors from individual reports. Often it is necessary to adjust reconnaissance positions considerably. In some cases, TIROS data are used to arrive at the "best track." This is particularly true in the central and eastern Atlantic. Comparisons were made only along that portion of the track for which there was sufficient conventional data to determine an accurate storm position independent of TIROS.

TIROS positions were obtained either from operational nephanalyses or from storm messages issued by the National Weather Satellite Center.

Storms used in this study are listed in Table 1 along with the number of TIROS fixes and range of error. A total of 54 storm positions were examined; 35 hurricanes, 9 tropical storms and 10 depressions. Fig. 1